Misan Journal of Engineering Sciences
Vol. 5, No. 1, 28 June 2026

ISSN: 2957-4242
ISSN-E: 2957-4250

Behaviour of Concrete-Filled Aluminium Columns with Curved Sections

Rawa L. Al-Jarosh[*1], Mohammed S. Abd Ali[*2]

[1]*Department of Civil Engineering, College of Engineering, University of Misan, Maysan, 62001, Iraq*
[1]*Department of Civil Engineering, Southern Technical University, Maysan, 62001, Iraq*
**Corresponding author E-mail:* rawalaith96@gmail.com

(Received 23 Dec 2025, Revised 12 Feb 2026, Accepted 19 Feb 2026)

Abstract: The structural performances of concrete-filled aluminium tubular (CFAT) stub columns with curved sections subjected to axial compression are studied using finite element modelling in the present investigation. The nonlinear properties of concrete and aluminium materials, along with the interactions among their components, are all taken into consideration while generating the finite element models. For concrete-filled aluminium tube columns with circular and rectangular sections, Zhou and Young (2008, 2009) obtained experimental ultimate strengths and load-axial strain relationships that is compared to the results obtained by finite element model. Various parametric analyses on essential materials and geometric features have been performed employing the validated finite element models. The mode of failure, load axial displacement relationship, and ultimate strength are investigated. The parametric investigation specimens are divided into four groups that present the influence of different parameters on the behaviour of a concert filled with short aluminium columns, which are cross-section shapes, aluminium proof stress, concrete cylinder strength, and tube thickness. To analyse the effect of cross-section parameter, these three sections—circular, elliptical, and round-ended—have been examined through first group. In the second group normal and high strength aluminium alloy are used in the tubes. Normal and high strength concrete effect are analysed in the third group. 1.9, 3, 5 mm thickness are investigated in the fourth group. To prevent overall column buckling, the lengths of the columns were selected to ensure that the ratio of length to diameter was consistently maintained at an approximate value of 3. Due to the outcomes, the circular cross-section had the greatest ultimate strength and ductility, therefore being the most desirable cross-section. A clear enhancement in ultimate load with increasing the aluminium proof stress, concrete cylinder strength, and aluminium wall thickness.

Keywords: Concrete filled aluminium columns; aluminium; Curved sections; CFRP; ABAQUS; Finite element analysis.

1. Introduction

Normally, Composite structures offer clear benefits and a flexible solution for matching various applications by combining two or more materials within a single member [1].

In structural applications, composite steel-concrete components are employed as an economical and fast construction technique [2]. Since the exterior steel tubes can be utilised as both permanent and integral formworks, saving labour costs, materials, and building time, this type of column is additionally proven to be affordable due to its rapid building process [3]. Investigations on composite aluminium-concrete elements have been reported, considering the advantages of structural aluminium's enhanced corrosion and strength-to-weight ratios [2].

Structural engineers have ignored aluminium based on a belief that it is a weak material, which is right as long as it is in pure form. An extremely strong alloy that avoids corrosion and weighs one-third of the weight of steel can be developed through mixing aluminium with particular components. According to the application, different aluminium alloys are used. It is a material that may be modified to satisfy certain requirements. Furthermore, in addition to being considered a green material when it comes to production and recycling, its strength and stiffness allowed the designer to minimise member sizes, reducing the building's overall cost [4].

DOI: https://doi.org/10.61263/mjes.v5i1.250

This work is licensed under a Creative Commons Attribution 4.0 International License.

Considering their strong anti-corrosion and aesthetic features, Aluminium alloys are becoming more common in building facades, footbridges, roofs and other constructions in humidity or corrosive conditions. [5].

However, since aluminium's Young's modulus (E) is only approximately 70 GPa, it could be sensitive to stability problems, which could harm the overall structural integrity. But this disadvantage could be overcome through enhancing the stiffness of structural aluminium elements with concrete. Concrete-filled empty sections of aluminium tube parts may enhance their stiffness and strength. Investigations on concrete-filled aluminium tubular (CFAT) columns are lacking, especially elliptical and round ended Which are may be required for architectural reasons, although there are multiple experimental data sets on the structural response of concrete-filled steel tubular (CFST) columns [6]. The current research analyses the structural performance of CFAT columns with curved sections through comparisons of circular, elliptical, and round-ended profiles, also study the impact of changing the concrete strength, aluminium proof stress, and tube thickness on the structural behaviour of composite columns.

The present research employs the finite element software ABAQUS 2019 for modelling concrete-filled aluminium columns numerically. The finite element simulation (FEM) took particular attention to the composite action between the concrete infill and the aluminium tube. The results of the experiments presented by Zhou and Young (2008, 2009) [7],[8] have been utilised to verify the finite element analysis (FEA) result. The impact of cross-section shapes and different parameters on the strengths of concrete-filled aluminium columns has been investigated by comprehensive parametric research. This research aims to providing a database to contribute later to improve standards of design concrete-aluminium composite columns with curved cross sections, improve their structural performance depending on design requirements, and motivate creative building techniques.

Concrete-filled hollow sections (tubes) were recently the focus of extensive investigation. The concrete core was contained by tubes constructed from steel, fibre-reinforced polymer, PVC, and various other materials [9], [10], [11]. Yet, little analysis has been carried out on aluminium tubes filled with concrete.

In 2006, Zhu and Young [12] investigated many hollow aluminium columns. The failure modes have tended to consist of local buckling, overall buckling, or the combination of local and overall buckling of columns.

In 2009, Zhou and Young [8] performed an experimental investigation of circular aluminium tube stub columns filled with concrete subjected to uniform axial compressive loads. The performance of these columns was researched using various tube diameters and concrete strengths (40, 70, and 100 MPa). The nominal proof stress of the aluminium elements was 240 MPa. The main variables of that research included the size of the aluminium tube and the strength of the concrete. The ratio of diameter to thickness was 9.7 - 59.7. The testing conclusions have been checked to those from the American and Australian/New Zealand standards. The outcomes of these specifications are usually moderate regarding these composite columns.

In 2012, Nasser [13] performed a theoretical and experimental investigation into the performance of circular aluminium tube columns that were filled with concrete under axial loading. The nominal proof stress of the aluminium components was 240 MPa. The key parameters during research were the diameter-to-thickness and length-to-diameter ratios. 24 specimens were manufactured and examined based on various D/t ratios range from 11.9 to 22.8, and L/D ratios range from 3 to 10.. In that research, empirical formulas have been proposed for estimating the strength of the columns. The mean value of the experimental-to-anticipated strength ratio was determined to be 1.0104.

Nasser [14], in 2014, performed a computational and experimental analysis of the structure behaviour of circular aluminium tube columns filled with concrete against increasing axial loading. The nominal proof stress of the chosen aluminium parts was 240 MPa. A fixed concrete strength of 24.2 MPa was employed to cast and test 24 specimens that had various ratios of D/t ($23.3 < D/t \leq 47.8$) and L/D ($3 \leq L/D \leq 10$). The maximum strength of the columns was estimated as well through a fuzzy inference system (FIS). The mean value of the experimental-to-estimated strength ratio has been found to be 1.001.

Jianqing et al. [15] in 2023, employed four specimens with different cross-sectional aspect ratios and cross-sectional aluminium contents to study the axial compression performance of concrete-filled circular-end aluminium tube (RECFAT) columns. Research results showed that local buckling of the aluminium tube plane produced oblique shear failure in a large number of specimens, though global instability failure showed up in specimens with an aspect ratio of 4.0. The round-ended aluminium tube's lateral strain formed more quickly, and the constraint effects were strongest when the aspect ratio approached 2.0.

A greater Axial load could be obtained by elliptical CFT columns with respect to rectangular and square CFT columns, corresponding to research on the elliptical CFT columns' ultimate strength performed by the writers using circular and square CFT columns by Giakoumelis and Lam [16] and Lam and Williams [17], with circular hollow sections offering greater confinement to the concrete core. This can be explained by the elliptical tube's curved section shape that raises circumferential tension and, thus, confines the concrete core more tightly. In other words, when CFT columns are under axial compression, the concrete core starts to expand lateral because of Poisson's effect. The curved aluminium tube limits this expansion through generating circumferential tension along the perimeter, which produces inward radial pressure (confinement) on the concrete.)

2. Finite Element Analysis

2.1. General

Laboratory investigations do not cover a wide range of variables since they require expensive devices and equipment, as well as a specialist laboratory with specially trained workers to carry out the procedures. Therefore, the most suitable choice to expand the range of parameters to be analysed is the finite element method (FEM). The strength and behaviour of concrete-filled aluminium columns under axial compression have been modelled by using a three-dimensional nonlinear numerical model.

2.2. Material modelling

2.2.1. Concrete

The confined concrete for CFAT columns is described with the concrete-damaged plasticity model, which is included in ABAQUS. Material parameters in this model could be calculated using formulae. Add the modulus of elasticity (E), dilation angle (Ψ), strain hardening-softening rule, ratio of compressive strength under biaxial loading to uniaxial compressive strength (fb0/fc0), and second stress invariant on the tensile meridian to that on the compressive meridian (Kc). Additional variables employed in ABAQUS involve the viscosity parameter (μ) and flow potential eccentricity (e).

Table 1 Concrete-damaged plasticity parameters

Ψ	E	fb0/fc0	Kc	μ
31	0.1	1.16	0.667	0.00002

2.2.2. Aluminium

This study used the computed stress-strain curves for the aluminium tubes that Zhou and Young [7] , [8]provided. In the multiaxial stress state, the Mises yield criteria with associated plastic flow are utilised. It is assumed that the aluminium alloy exhibits isotropic hardening behaviour. The PLASTIC selection in ABAQUS gives material behaviour that makes it possible to employ a multi-linear stress-strain curve. The elastic region up to the proportional limit stress is expressed by the first section of the multi-linear curve, having a measured Young's modulus and Poisson's ratio of 0.33. The nominal (engineering) static stress-strain curve has been m4odified into a true stress and logarithmic plastic strain curve since the analysis contains high inelastic strains. ABAQUS provides the log plastic strain (ε_{ln}^{pl})and true stress (σ_{true}).

2.2.3. CFRP Properties

To enhance the final performance of the composite columns, the features of Carbon Fiber Reinforced Polymer (CFRP) have been included in the numerical model identical to an experimental study. The primary aim for utilising CFRP wrapping at the top and bottom of the columns is to delay or avoid local buckling, also referred to as "elephant foot failure", which usually occurs due to large compressive stresses and leads to instability at the column's base [18], it also doesn’t have major impact on the results. The height of the CFRP varied based on the column height.

2.2.4. Steel

The steel plates installed at each specimen's ends have been defined. The top plate acted as a loading plate that transmitted the applied axial load equally to the column cross-section, while the bottom plate served as a support plate that offered a stable foundation and allowed uniform stress distribution over the boundary conditions. As was common in finite element simulation, it was assumed that the steel material had a constant elastic response during the study, as the plates were not involved in the loading or the structural system that was being studied.

2.3. Element type and mesh

The ABAQUS (2019) element library was utilised to determine composite column element types. The concrete core, support plates, and loading plates are simulated through the three-dimensional eight-node solid elements (C3D8). The aluminium tubes and CFRP are simulated through the four-node shell element with reduced integration (S4R). Convergence studies are applied to identify the mesh sizes in order to provide reliable simulations with the least amount of additional computing consumption. To get accurate outcomes, the probable grid size of each part was selected based on the specimen dimensions. Figure 1 displays typical specimens with meshes.

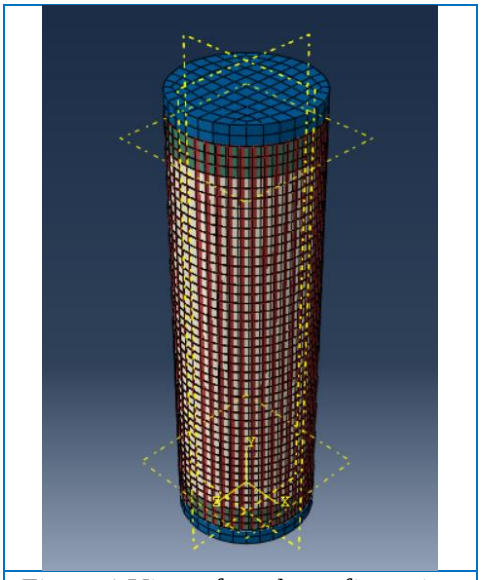


Figure 1 View of mesh configuration

2.4. Interaction and Boundary Conditions

A tie constraint was used to connect the aluminium edges and the plate edges, in addition to connecting the loading and supporting plates with the concrete core. For the interface between the aluminium tube and the concrete core, a surface-to-surface interaction was chosen. Hard contact arises in the normal direction of two surfaces interacting. A penalty function with a friction coefficient of 0.4 was chosen for study in the tangential direction.

The supporting plate's bottom surface was bound towards all degrees of freedom throughout the test process. The displacement is generated at the loading plate's top layer in the direction of the load being applied. The experiments and the model with finite elements (FEM) both adopted a similar loading procedure. The concrete-filled aluminium columns were studied by applying the displacement control procedure. The specimen was tested to an equal vertical compressive uniform load by applying a displacement at each node of the laden end on the top surface.

3. VALIDATION OF STUDY MODEL

3.1. Overview of experimental research

Results of previous investigations carried out by other researchers for concrete-filled aluminium tube columns using circular and rectangular sections were compared with the results of the present FE model employing ABAQUS (2019) to check the current FE model utilised in the present research.

To achieve this objective, four specimens were chosen: two rectangular sections from Zhou and Young [7] and two circular sections from Zhou and Young [8]. The measurements and material features for the above specimens are presented in the Tables (2, 3). Testing was carried out on the hollow sections created through extrusion employing 6061-T6 treated with heat alloy of aluminium (a high-strength materials) together with concrete filling.

To reduce overall column buckling, the total length of the column (L) was selected to ensure the length-to-diameter ratio (L/D) of the concrete-filled aluminium stub columns was commonly kept at a fixed value of 3. Concrete cylinder with nominal strengths of 40 and 70 MPa were employed to test the column samples. The concrete strength is marked by the letter "C" in the series label, which is followed by the nominal concrete cylinder strength in MPa.

Table 2 Summarize of the CHS column test [8]

Specimen	Diameter, D (mm)	Thickness, T (mm)	D/t	Length, L (mm)	L/D	Aluminium tube, fy (MPa)	Concrete, fc (MPa)
CHS7C40	150.1	2.53	59.3	450	3	267.9	44.8
CHS7C70	150.1	2.54	59.1	451	3	267.9	70.2

Table 3 Summarize of the RHS column test [7]

Specimen	Depth, D (mm)	Width, B (mm)	Thickness, T (mm)	D/t	Length, L (mm)	L/D	Aluminium tube fy (MPa)	Concrete, fc (MPa)
RHS1C40	100	44.1	1.57	63.8	300	3	263	36.1
RHS1C70	100	44.1	1.57	63.7	300	3	263	74.4

3.2. Comparison between experimental and FEA results

Here, the ultimate load capacity and the load-axial strain are two measurements which are utilised to analyse and compare the present model with experimental studies. Analysing and verifying the finite element design's validity is the main aim of this comparison.

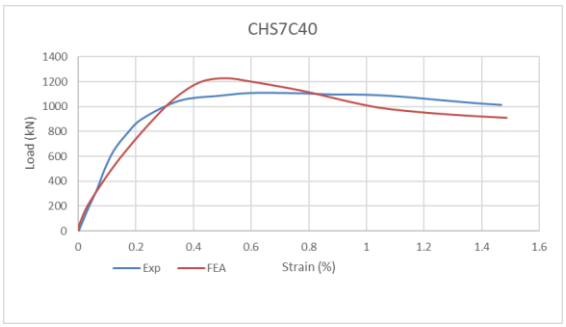
Initially, Table 4 clearly illustrates the good agreement with the results produced by the ABAQUS (2019) model and experimental research for ultimate load capacity. The experimental and numerical results for the specimens indicated an upper limit difference of 10%.

Table 4 Verification of finite element model

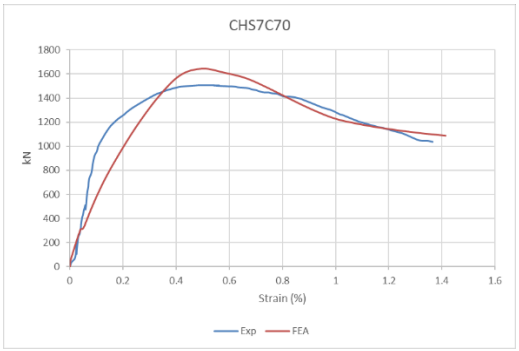
Specimen	D/t	P_{Exp} (KN)	P_{FEA}(KN)	P_{Exp}/P_{FEA}
CHS7C40	59.3	1111.1	1228.63	0.9
CHS7C70	59.1	1496.4	1643.18	0.91
RHS1C40	63.8	182	193.847	0.94
RHS1C70	63.7	296	296.595	0.99

Four concrete-filled aluminium tube specimens were selected depending on the available experimental data, and their load-strain behaviour was also evaluated. The load-strain relationship comparing the experimental and proposed FE model is displayed in Figure 2.

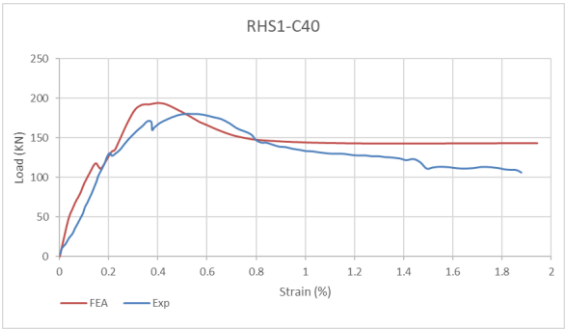
The provided current model format presents an amazing high standard for its experiment match, and the present model effectively shows the relationship between load and strain. It can also be illustrated how the FE current model correlates with experiment through elastic and plastic phases.



(A) CHS7C40



(B) CHS7C70



(C) RHS1C40



(D) RHS1C70

Figure 2 Experimental versus current FE model for columns

4. PARAMETRIC STUDY

The present study uses the existing finite element model to simulate concrete-filled aluminium tube columns that have different parameters, based on interesting results compared to laboratory testing.

A parametric investigation was done to study the impact of cross-sectional shapes and various parameters on the strength of concrete-filled aluminium columns. Four groups of composite columns with different parameters are analysed.

In the first group Three cross-sections were examined on concrete-aluminium composite columns. For the comparison, three different cross sections (circular, elliptical, and round-ended) as shown in Figure 3 of CFAT were developed. It was demonstrated that each specimen in the circular section with specific thickness, area, and length have an equivalent specimen in the opposite elliptical and round ended section specimens. Therefore, the first group involves three equivalent specimens to compare them. The second group investigated the effects of different aluminium proof stresses, which are 267.9 and 185.9Mpa. The third group investigated the effects of different strengths of the cylindrical concrete, which are 44.8 and 70.2Mpa. The fourth group analyses the effect of different aluminium wall thicknesses, which are (1.9, 3, and 5 mm).

The dimensions of the cross-section and the strengths of the concrete-filled aluminium columns, determined by the finite element analysis (FEA), are presented in Tables 6-9. The experimentally determined material characteristics of the concrete core and aluminium tubes by [8], [19] were employed in this parametric investigation. Table 5 explained properties for 6061-T6 and 6063-T5 aluminium alloys. The (6061-T6 high-strength, heat-treated aluminium alloy) tube's (series CHS7) nonlinear stress-strain curve, measured by [8], with a 267.9 MP a yield stress, was employed in the parametric analysis for aluminium tubes for all groups. The (6063-T5 normal-strength, heat-treated aluminium alloy) tube's (N-C2-NW) nonlinear stress-strain curve, measured [19], with a 185.9 MP a yield stress, was employed in the parametric analysis for aluminium tubes for the second group. For specimens in all groups, the compressive concrete cylinder strength equal to 44.8MPa, as presented by [8], was adopted for the concrete infill. On the other hand, for specimens of group

three, the compressive concrete cylinder strength of 70.2 MPa, as presented by [8] was adopted for the concrete infill.

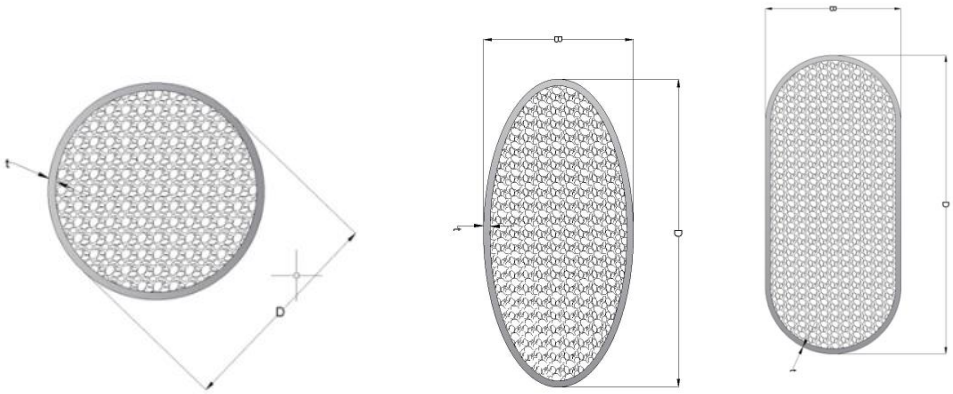


Figure 3 Specimens shapes.

Table 5 Aluminium property of parametric study [8][19]

Aluminium alloy	E_0 (GPa)	$\sigma_{0.2}$(MPa)	σ_u(MPa)	ε_f(%)
6063-T5	67.1	185.9	207.7	10.4
6061-T6	64.9	267.9	282.9	10.1

4.1. Specimen labelling

The column for test specimens is marked to denote the aluminium proof stress, cross-section shape, aluminium tube wall thickness, and the strength of the nominal concrete cylinder. The name labelling is explained below:

- T6 indicates 6061-T6 (high-strength material) heat-treated aluminium alloy, and T5 indicates 6063-T5 (normal-strength material) heat-treated aluminium alloy.
- Second letters are identifying the aluminium tube cross-section shape, with (C) indicating the circular hollow section.
- The second number specifies the aluminium tube thickness, where 2 indicate 2mm wall thickness.
- The designations (C70) and (C40) refer to concrete cylinder strength, where (C70) represents (=70.2MPa), and (C40) representing (=44.8MPa).

4.2. Ductility Index

In structural engineering, ductility is an important measure of how effectively columns work. It describes how efficiently a member can handle a lot of plastic deformation without losing its ability to bear weight or structural rigidity all of a sudden. [20]

The ductility index can be calculated using the load-displacement curve by divided the (Δ0.85) by (Δu). as shown in Figure (4). Thus, the ductility is obtained by Equation below. [21]

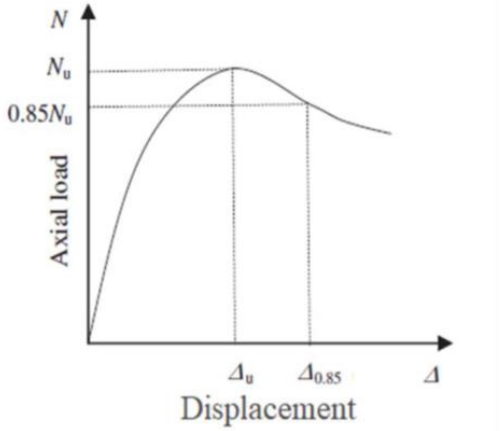


Figure 4 Illustrate of ductility index. [21]

5. Test results and discussion

The relationship of load with axial displacement, in addition to the test strengths, was determined for the column specimens. The test strengths (P_{FEA}) of the concrete-filled aluminium stub columns are given in Tables 6-9.

At first, for group one the Table 6 indicates that circular cross-sections always outperformed the remaining geometric shapes regarding the ultimate load capacity for all of the different diameter-to-thickness ratios that were studied. A column having a circular cross-section provides greater structural efficiency as well as uniform load distribution when compared to various cross- section types. Loading stresses in circular cross-section columns have equal distribution across the entire perimeter.

The columns having elliptical cross-sections (T6E2C40, T6E3C40, T6E4C40) exhibited ultimate load decreases of 6%, 5%, and 3%, respectively, compared with their circular reference equivalents. The small decreases come due to the elliptical shape's lower consistency in curvature, which slightly lowers the smallest moment of inertia in the major axis direction and induces uneven stress distribution.

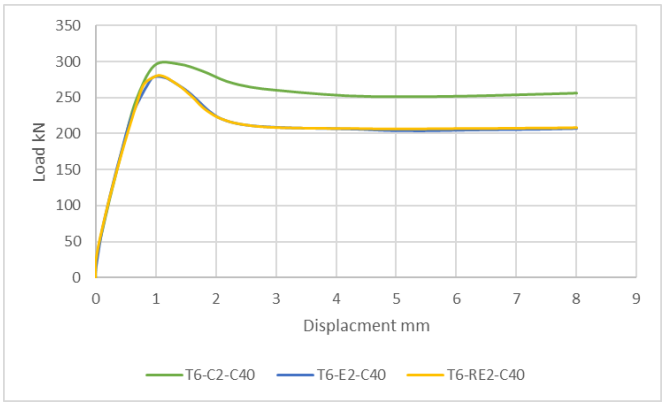
The columns having round-ended cross-sections (T6RE2C40, T6RE3C40, T6RE4C40) exhibited decreases of 5%, 4%, and 4%, respectively, compared with their circular reference equivalents. The rounded ends improve performance by lowering the concentration of stress at corners; however, elliptical and round ended cross-sections columns remain less efficient compared to complete circular shape columns.

Table 6 Specimen dimensions and results of group one.

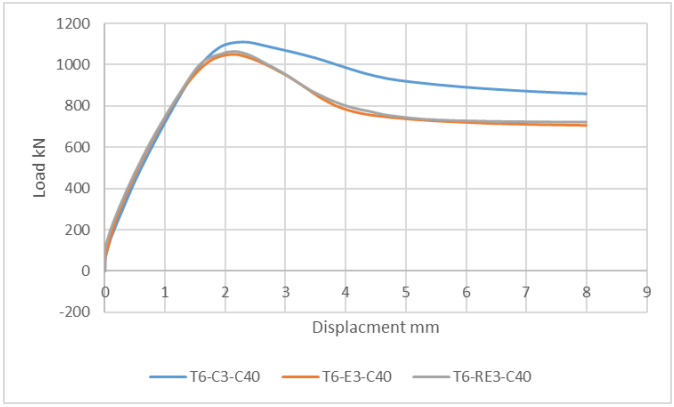
Specimen	D (mm)	B (mm)	Thickness, t (mm)	Length, L (mm)	$\frac{D}{t}$	$\frac{L}{D}$	A (mm^2)	Load Capacity, $P_{FEA\,(KN)}$	DI	Change %
T6C2C40	66	-	2	215	33	3.25	3421.2	297.043	3.03	0
T6C3C40	135	-	3	440	45	3.25	14313.9	1109.89	1.99	0
T6C4C40	235	-	4	765	58.7	3.25	43373.7	3027.48	1.8	0
T6E2C40	93.3	46.6	2	215	46.6	2.3	3420.5	279.69	1.77	-41.6
T6E3C40	190.9	95.4	3	440	63.6	2.3	14313.6	1051.8	1.58	-20
T6E4C40	332.3	166.2	4	765	83	2.3	43373.6	2933.8	1.51	-16
T6RE2C40	87.5	43.7	2	215	43.7	2.45	3418.9	280.69	1.65	-45.5
T6RE3C40	179.1	89.5	3	440	59.6	2.45	14311.1	1064.78	1.55	-22
T6RE4C40	311.7	155.8	4	765	77.9	2.45	43371.5	2911.03	1.49	-17

From load-axial displacement curves as shown in Figure 5 can determined the DI for the columns. Table 6 proved ductility index significantly decrease with elliptical sections (T6E2C40, T6E3C40, T6E4C40) with decreasing in ductility index of (1.77, 1.58, 1.51) specifically by (41.6%, 20%, 16%) respectively lower than circular section control columns (T6C2C40, T6C3C40, T6C4C40). The ductility index also decreases with round-ended section columns (T6RE2C40, T6RE3C40, T6RE4C40) with decreasing in ductility index of (1.66, 1.55, 1.49) specifically by (45.5%, 22%, 17%) respectively lower than circular section control columns (T6C2C40, T6C3C40, T6C4C40).

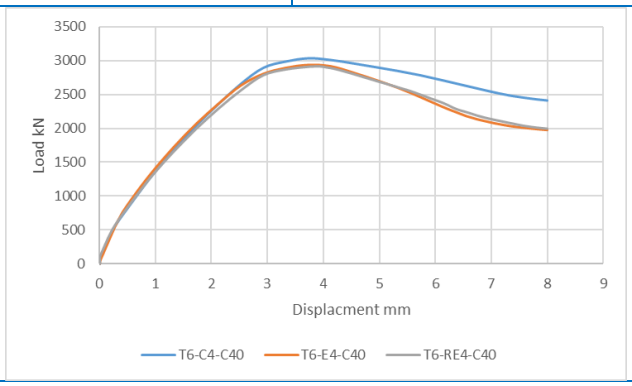
ISSN: 2957-4242
ISSN-E: 2957-4250



(A)



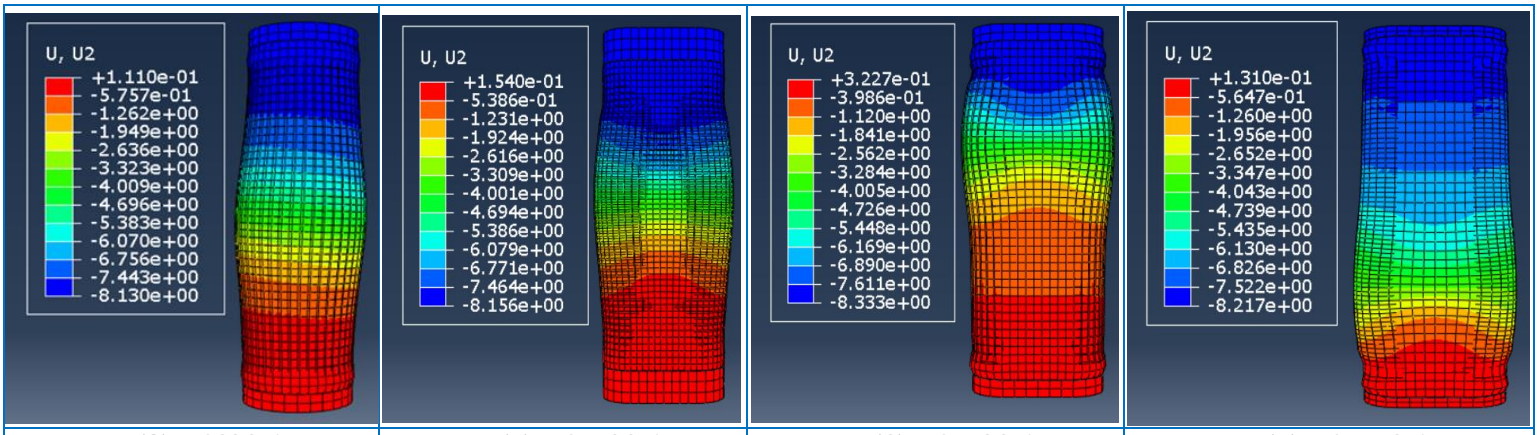
(B)



(C)

Figure 5 Load-axial strain relationship for group one

All the specimens with circular cross-section exhibited outward local buckling within the middle of the column height, with one exception for column T6C3C40, which failed in shear mode. In columns having elliptical cross-sections, local buckling usually starts at the middle of the column height. Round-ended section columns exhibited local buckling at different places across the column's height, dependent on the D/t ratio as shown in Figure 6 Where the contour colours refer to axial displacement (u2) as it is symbolised in the program. The local buckling position is determined by the lateral deformation.



(A) T6C3C40 | **(B) T6RE2C40** | **(C) T6RE3C40** | **(D) T6RE4C40**

Figure 6 Failure modes

For group two, Table 7 illustrates a clear increase in ultimate load-carrying capacity of tested specimens as rises of aluminium proof stress rises from 185.9 to 267.9 MPa. The (T6C2C40, T6C3C40, T6C4C40) specimens having aluminium proof stress equal to 267.9 MPa, displayed an increase in ultimate load of 20%,

17%, and 14% respectively, when compared to columns (T5C2C40, T5C3C40, T5C4C40) that had aluminium proof stress equal to 185.9 MPa. This improvement comes from the enhanced proof stress, resulting in better resistance to initial yielding and deformation against compressive loads, in turn delaying the start of modes of failure such as local buckling or crushing.

Table 7 Specimen dimensions and results of group two.

Specimen	f_y	D (mm)	t (mm)	L (mm)	$\frac{D}{t}$	$\frac{L}{D}$	A (mm^2)	Load Capacity, $P_{FEA\ (KN)}$	DI	Change %
T5C2C40	185.9	66	2	215	33	3.25	3421.2	246.5	2.72	0
T5C3C40	185.9	135	3	440	45	3.25	14313.9	944.6	1.72	0
T5C4C40	185.9	235	4	765	58.7	3.25	43373.7	2649.4	1.65	0
T6C2C40	267.9	66	2	215	33	3.25	3421.2	297	3.03	+ 11
T6C3C40	267.9	135	3	440	45	3.25	14313.9	1109	1.99	+ 16
T6C4C40	267.9	235	4	765	58.7	3.25	43373.7	3027	1.8	+ 8

Table 7 proved that with increasing the aluminium proof stress from 185.9 to 267.9MPa the ductility index slightly enhances with circular-section columns (T6C2C40, T6C3C40, T6C4C40) with increasing in ductility index of (3.03, 1.99, 1.8) specifically by (11%, 16%, 8%) respectively higher than circular section control columns having aluminium proof stress equal to 185.9MPa namely (T5C2C40, T5C3C40, T5C4C40).

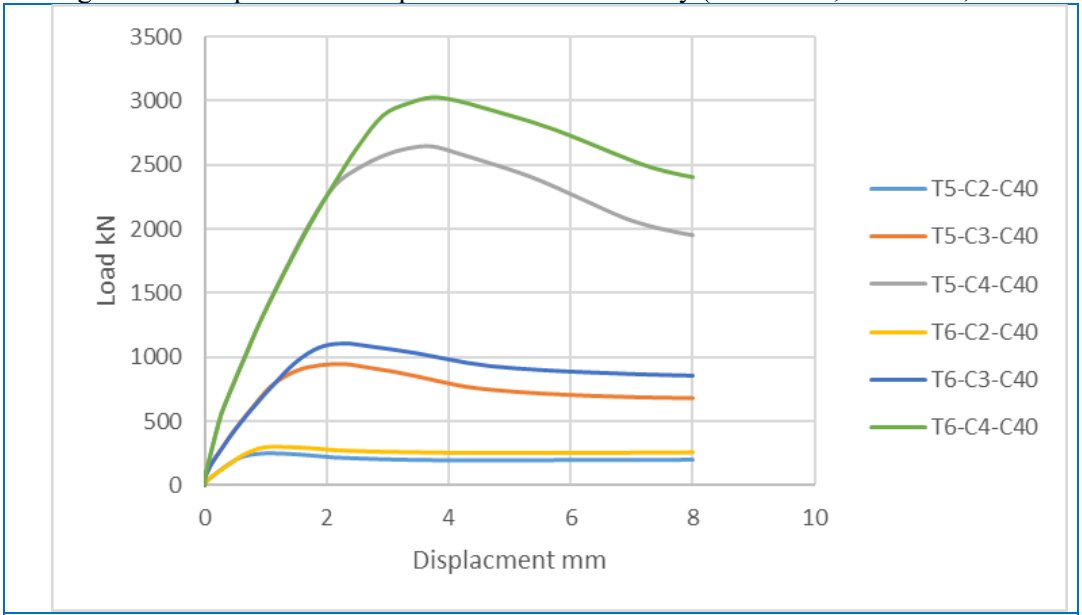


Figure 7 Load-axial strain relationship for group two

In circular cross-sections, local buckling often occurred in the middle height of the column across all specimens, because of the concentration of inelastic strains and geometric weaknesses under compressive pressures.

Notable exceptions have been observed in circular cross-sections T5C3C40 (= 185.9 MPa) and T6C3C40 (f_y = 267.9 MPa), in addition to in the specimen T5C2C40 (= 185.9 MPa), where shear failure dominated as shown in Figure 8. The differences are caused by not enough lateral confinement provided by the aluminium tube, leading to early shear band formation before local buckling, particularly in sections with an intermediate value of (D/t = 45) ratio, which show reduced post-yield ductility and greater sensitivity to shear stresses.

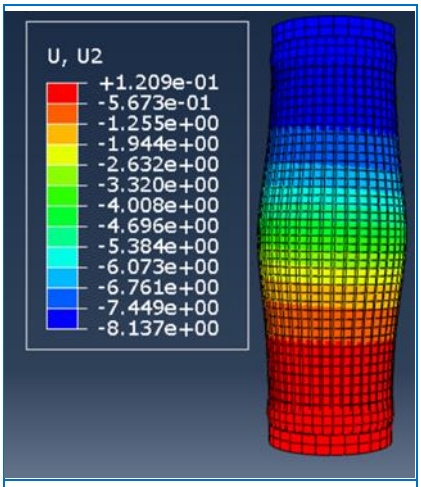


Figure 8 Failure mode for T5C3C40

For group three, Table 8. Indicate The columns having a concrete compressive strength equal to 70MPa, displayed an increase in ultimate load of 25%, 28%, and 33% for ((T6C2C70, T6C3C70, T6C4C70)) sections, respectively, when compared to columns that had concrete compressive strength equal to 40MPa. Enhancement comes from the key function of concrete compressive strength to determine concrete's axial and confining capacities, as higher-strength concrete provides stronger resistance to compressive stress.

Table 8 Specimen dimensions and results of group three.

Specimen	f'_c	D (mm)	t (mm)	L (mm)	$\frac{D}{t}$	$\frac{L}{D}$	A (mm^2)	Load Capacity, $P_{FEA\,(KN)}$	DI	Change %
T6C2C40	44.8	66	2	215	33	3.25	3421.2	297	3.03	0
T6C3C40	44.8	135	3	440	45	3.25	14313.9	1109	1.99	0
T6C4C40	44.8	235	4	765	58.7	3.25	43373.7	3027	1.8	0
T6C2C70	70.2	66	2	215	33	3.25	3421.2	374	1.94	- 36
T6C3C70	70.2	135	3	440	45	3.25	14313.9	1425	1.76	- 11
T6C4C70	70.2	235	4	765	58.7	3.25	43373.7	4031	1.62	- 9

On the other hand, ductility index was reduced in the samples that had increasing concrete infill strengths, namely from grade 40 to 70MPa. Can be noticeable with columns (T6C2C70, T6C3C70, T6C4C70) with decreasing in ductility index of (1.94, 1.76, 1.62) specifically by (-36%, -11%, -9%) respectively lower than control columns having concrete compressive strengths equal to 40MPa namely (T6C2C40, T6C3C40, T6C4C40). It was observed that there was a major difference in curves throughout columns with high-strength infilled compared to those with normal-strength infilled. When the high-strength concrete core reaches its ultimate load, the aluminium tube around it approaches its yield point. On the other hand, within specimens with normal strength filling, the aluminium tube achieves yield stresses early from the concrete-filled reaching ultimate load.

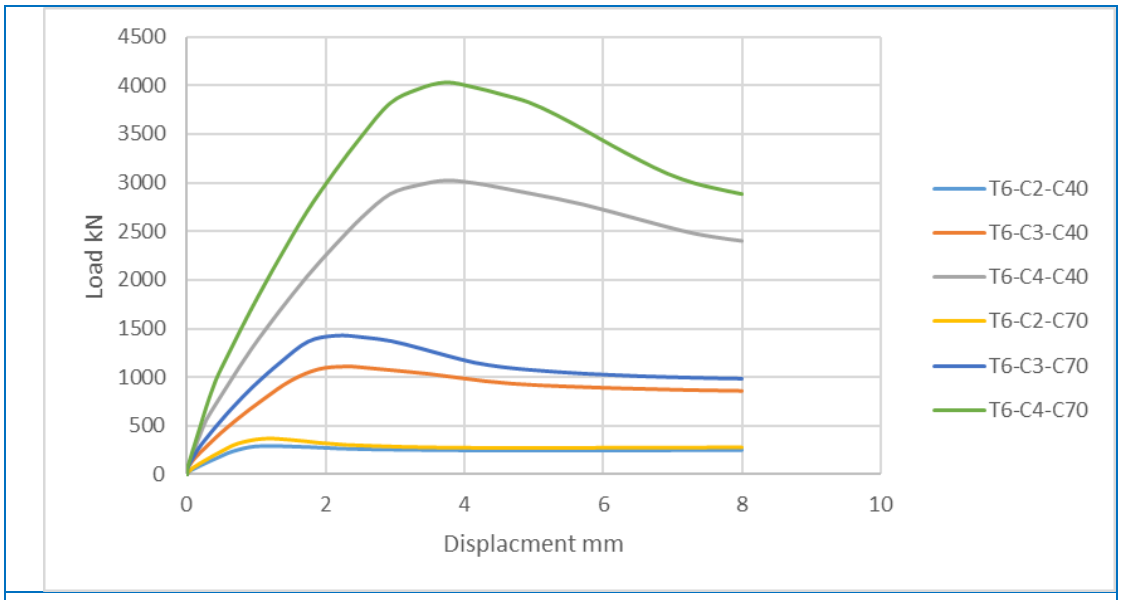


Figure 9 Load-axial strain relationship for group three.

In circular cross-sections, local buckling often occurred in the middle height of the column across all specimens, because of the concentration of inelastic strains and geometric weaknesses under compressive pressures.

Exceptions occurred in T6C3C40, T6C3C70, and T6C2C70, that shear failure occurred as shown in Figure 6(A). The difference is caused by increased concrete confinement with higher-strength concrete, which delays local buckling by enhancing the tube's lateral confinement (through the concrete-core expansion effect), thus enabling shear-dominated failure, which includes diagonal cracking and decreasing post-yield ductility.

For group four, for columns that had an aluminium wall thickness of 3 mm, 5mm the ultimate load increased about 22%, 58%, respectively compared with columns having a wall thickness of 1.9 mm. This gradual improvement is caused by more resistance to local buckling and higher material stiffness of the walls with greater thickness, which better activates the composite action that occurs between the aluminium wall and filling under the axial compression.

Table 9 Specimen dimensions and results of group four.

Specimen	D (mm)	t (mm)	L (mm)	$\frac{D}{t}$	$\frac{L}{D}$	A (mm^2)	Load Capacity, $P_{FEA\ (KN)}$	DI	Change %
T6C5C40	135	5	440	27	3.25	14313.9	1435.3	3.1	+ 67
T6C3C40	135	3	440	45	3.25	14313.9	1109	1.99	+ 7
T6C1.9C40	135	1.9	440	71	3.25	14313.9	907.5	1.86	0

Table 9 proved ductility index highly enhances with columns having 3mm, 5 mm wall thickness (T6C3C40, T6C5C40) with increasing in ductility index of (1.99,3.1) specifically by (7%, 67%) higher than circular section control column with a 1.9mm wall thickness (T6C1.9C40).

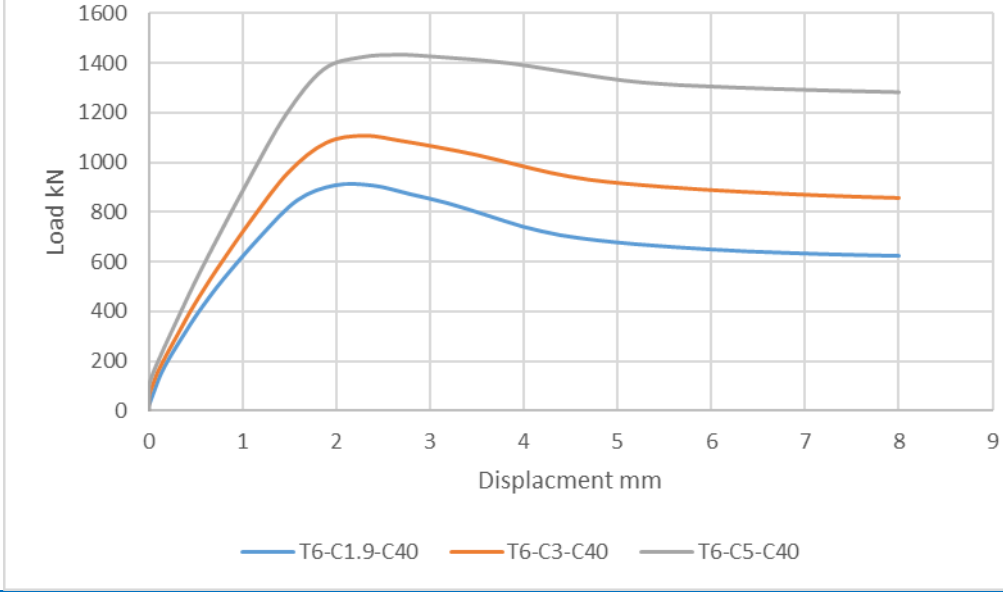


Figure 10 Load-axial strain relationship for group four.

Circular cross-section columns limited by 1.9 mm and 3 mm thick walls exhibited failure of shear at the middle height. This behaviour develops because of insufficient lateral confinement, therefore is not prevent shear banding, a localised shear deformation mode observed in unconfined thin components under axial forces.

On the other hand, column having a 5 mm thickness of aluminium displayed ductile "drum-like" deformation indicated by bending at middle height where the outer diameter exceeds that at the ends, absent of local buckling indication as shown in Figure 11. The improvement in confinement stiffness resulting from a thicker wall provides greater radial constraint, increasing the critical buckling stress, leading to stable, post-elastic expansion instead of instability.

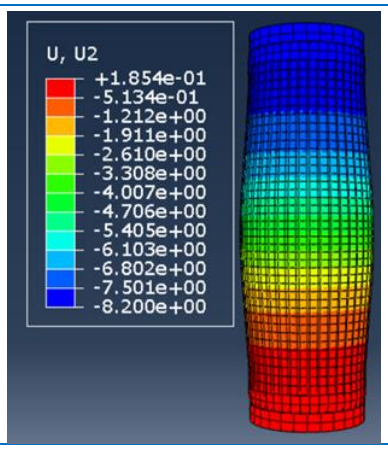


Figure 11 Failure mode for T6C5C40

6. CONCLUSION

The study displays the finite element model (FEM) of concrete-filled aluminium tube columns with curved cross sections under axial compression force. Previous data from experiments were employed to verify the accuracy of the proposed model by comparing ultimate load capacity and load-axial strain curves. The study showed that the used model produced reliable outcomes in analysing the behaviour of concrete-filled aluminium tube columns with circular and rectangular cross-sections, showing a high comparability range between 0.90 and 0.99. The close correlation established through the experimental and performed finite element model encourages an additional deep examination of modelled curved cross sections.

It is noted that:

- ABAQUS, a finite element modelling application, is utilised for developing finite element models of CFAT stub columns under axial compression. An aluminium tube, a concrete core, and the interface between them are the three primary components of the model. Favourable correlations were developed between the experimental and finite element research with respect to ultimate strengths and the load-axial strain relationship.
- The circular cross-section proved greater efficiency, which shows its highest ultimate strength and ductility.
- Local buckling was mostly detected in the centre position, except for the rounded ends, which displayed different local buckling locations according to the (D/t) ratio.
- For circular shapes, columns that display aluminium proof stress increased from 185.9 MPa to 267.9 MPa, and an increase in the ultimate load was observed, ranging from 14% ,17%, 20%. This range depends on the nonlinear relationship between the ultimate load and the (D/t) ratio, where the highest increase in ultimate load was noticed in the lowest (D/t) ratio columns.
- For the rising of compressive strength of the concrete core from (40MPa) to (70 MPa), there was a clear increase in the ultimate load, ranging between 25%, 28%, and 36%. This range relies on the linear relation discovered between the ultimate load and the ratio of (D/t); the largest rise in ultimate load is achieved in slender section columns
- A clear enhancement in ultimate load with increasing the aluminium wall thickness. The incremental advancement is caused by greater resistance to local buckling and enhanced material stiffness of walls that are thicker, which effectively activates the interaction between the aluminium shell and infill material beneath axial compression.

Author Contributions: The authors contributed to all parts of the current study.
Funding: This study received no external funding.
Conflicts of Interest: The authors declare no conflict of interest.

References

[1] S. F. Resan, ‘Behavior of aluminum columns enhanced with CFRP and filled by light weight concrete’, *Engineering and Technology Journal*, vol. 32, no. 11, pp. 2658–2672.

[2] M. Gkantou, E. Georgantzia, A. Kadhim, G. S. Kamaris, and M. Sadique, ‘Geopolymer concrete-filled aluminium alloy tubular cross-sections. Structures 51: 528–543’, 2023.

[3] N. Jamaluddin, D. Lam, X. H. Dai, and J. Ye, ‘An experimental study on elliptical concrete filled columns under axial compression’, *J. Constr. Steel Res.*, vol. 87, pp. 6–16, 2013.

[4] G. Nayak, K. K. Shetty, and S. Abdalla, ‘Effect of depth to thickness ratio and length to depth ratio on hollow section aluminium tubes filled with self-compacting concrete’, *Int. J. Res. Eng. Technol.*, vol. 3, no. 3, pp. 675–678, 2014.

[5] F.-C. Wang, H.-Y. Zhao, and L.-H. Han, ‘Analytical behavior of concrete-filled aluminum tubular stub columns under axial compression’, *Thin-Walled Structures*, vol. 140, pp. 21–30, 2019.

[6] E. Georgantzia, S. Bin Ali, M. Gkantou, G. S. Kamaris, K. Kansara, and W. Atherton, ‘Structural response of aluminium alloy concrete filled tubular columns’, *ce/papers*, vol. 4, no. 2–4, pp. 614–620, 2021.

[7] F. Zhou and B. Young, ‘Tests of concrete-filled aluminum stub columns’, *Thin-Walled Structures*, vol. 46, no. 6, pp. 573–583, 2008.

[8] F. Zhou and B. Young, 'Concrete-filled aluminum circular hollow section column tests', *Thin-Walled Structures*, vol. 47, no. 11, pp. 1272–1280, 2009.

[9] saadoon A. S., 'Experimental and theoretical investigation on PVC-concrete composite columns', Ph. D. Dissertation , University of Basrah , Basrah, Iraq, 2010.

[10] D. Lam and K. K. Y. Wong, 'Axial capacity of concrete filled stainless steel columns', in *Structures Congress 2005: Metropolis and Beyond*, 2005, pp. 1–11.

[11] W.-K. Hong and H.-C. Kim, 'Behavior of concrete columns confined by carbon composite tubes', *Canadian Journal of Civil Engineering*, vol. 31, no. 2, pp. 178–188, 2004.

[12] J.-H. Zhu and B. Young, 'Tests and design of aluminum alloy compression members', *Journal of structural engineering*, vol. 132, no. 7, pp. 1096–1107, 2006.

[13] K. Z. Nasser, 'Structural behavior of concrete filled aluminum tubular columns', *Basrah Journal for Engineering Science*, vol. 12, no. 1, pp. 46–49, 2012.

[14] K. Z. Nasser, 'Experimental and Computational Study of Concret Fill Aluminum Tubular Column Under Axial Loads', *Kufa Journal of Engineering*, vol. 5, no. 2, pp. 29–46, 2014.

[15] J. Bu, Q. Liu, Y. Yu, and Q. Qiu, 'Axial compression performance and bearing capacity calculation of round-ended concrete-filled aluminum tube column', *Applied Sciences*, vol. 13, no. 13, p. 7918, 2023.

[16] G. Giakoumelis and D. Lam, 'Axial capacity of circular concrete-filled tube columns', *J. Constr. Steel Res.*, vol. 60, no. 7, pp. 1049–1068, 2004.

[17] D. Lam and C. A. Williams, 'Experimental study on concrete filled square hollow sections', *Steel and Composite Structures, An International Journal*, vol. 4, no. 2, pp. 95–112, 2004.

[18] U. Brian, 'Local and postlocal buckling of fabricated steel and composite cross sections', *Journal of Structural Engineering*, vol. 127, no. 6, pp. 666–677, 2001.

[19] J.-H. Zhu and B. Young, 'Experimental investigation of aluminum alloy circular hollow section columns', *Eng. Struct.*, vol. 28, no. 2, pp. 207–215, 2006.

[20] T. Sheehan, 'Cyclic behaviour of hollow and concrete-filled circular hollow section braces', Doctoral dissertation, University of Warwick, 2013.

[21] N. Jamaluddin, 'Behaviour of elliptical concrete-filled steel tube (CFT) columns under axial compression load', Doctoral dissertation, University of Leeds, 2011.